# Covalent Bonding and Spin Density in *cis*-$[Fe(bipy)_2Cl_2][FeCl_4]$ (bipy = 2,2′-Bipyridyl) studied by Polarised Neutron Diffraction†

**Brian N. Figgis* and Philip A. Reynolds**
*School of Chemistry, University of Western Australia, Nedlands, W.A. 6009, Australia*
**J. Bruce Forsyth**
*Rutherford-Appleton Laboratory, Didcot, Oxon, OX11 0QX*

Polarised neutron-diffraction experiments on the *Pccn* polymorph of deuteriated *cis*-$[Fe^{III}(bipy)_2Cl_2][Fe^{III}Cl_4]$ (bipy = 2,2′-bipyridyl) gave 402 unique magnetic structure factors collected with magnetic fields almost parallel to the *c* and *b* crystal directions. These data were analysed using a valence-orbital model involving anisotropic spin populations on all non-hydrogen atoms. The model refined to $R' = 0.052$ and $\chi = 1.56$. Most of the spin resides on the iron atoms. In the cation the populations are Fe 3*d* 4.38(15), 4*p* −0.60(15), in the anion Fe 3*d* 4.13(15), 4*p* 0.00(17). Approximately 0.23 spins reside on each chlorine atom and 0.34 on each bipyridyl molecule of the cation. In the $[FeCl_4]^-$ anion the division between 3*d* $t_2$ and 3*d* *e* populations on the iron(III) atom, $3p_\sigma$ and $3p_\pi$ populations on the chlorine atoms, and overlap density in the Fe–Cl bonds show the spin delocalised onto the chlorine atoms *via* both $e^*$ and $t_2^*$ molecular orbitals with approximately equal amounts of σ and π spin transfer. There is significant 4*p* participation in the $t_2^*$ molecular orbital. In the $[Fe(bipy)_2Cl_2]^+$ cation the Fe–Cl bonding is similar to that in the anion. The bidentate 2,2′-bipyridyl ligand has much more spin in the ring bonded by the shorter Fe–N bond, 0.25(3), than on the other ring, 0.09(3), with σ donation into $3d_\sigma$ and π back-donation from the iron 3*d* $t_{2g}$ orbitals. The distribution agrees qualitatively, but not quantitatively, with the charge-density results and theoretical predictions. Comparison with charge-density results shows that besides covalent spin transfer there are spin-polarisation effects, arising from electron–electron correlation, of similar size. These effects complicate simple molecular orbital descriptions of the bonding in both cation and anion of the complex, but agree with theoretical conclusions developed for the $[CoCl_4]^{2-}$ ion.

Covalent bonding in transition-metal complexes has been much studied by spectroscopic and other techniques such as magnetic susceptibility and e.s.r. measurements, which probe their *energetic* properties. Diffraction methods, which probe the *spatial* distribution of electrons, provide a different perspective. This spatial information provides a direct observation of spin and charge transfers due to covalence, and unambiguous evidence on these is difficult to extract from spectroscopic and related experiments. *X*-Ray diffraction allows us to measure the charge-density distribution in detail, thus directly examining the changes which result on chemical bonding. The spin density is more sensitive to bonding effects than is the charge density because the core orbitals are formally spin-paired and do not contribute much to the spin. For suitable ions, those with large magnetisation at a temperature of 4.2 K and a magnetic field of 4.6 T, say, and an orbitally non-degenerate ground state, we can measure the spin density by means of the polarised neutron diffraction (p.n.d.) experiment.

The technique of p.n.d. has provided a number of detailed studies of the spin density in paramagnetic first-transition series metal complexes, for example $Cs_3[CoCl_4]Cl$,[1] $Rb_2[CrCl_4]$,[2] and $Cs_2K[Cr(CN)_6]$.[3] Especially when combined with the charge-density studies using the *X*-ray experiment, these have provided a uniquely detailed probe of metal–ligand bonding interactions.

Because of the large amount of data required adequately to describe the magnetisation density, larger complexes have been little studied by the p.n.d. technique. The exceptions are the relatively low accuracy studies of the phthalocyanine derivatives of manganese[4] and cobalt.[5] We have now undertaken a study of the large complex $[Fe(bipy)_2Cl_2][FeCl_4]$ of $Fe^{III}$ (bipy- = 2,2′-bipyridyl)[6] to determine if current analysis techniques can provide useful information from the limited but accurate p.n.d. data sets obtainable from crystals of such complexity.

The compound $[Fe(bipy)_2Cl_2][FeCl_4]$ can be crystallised as the orthorhombic *Pccn* polymorph. The structure of the deuteriated material has been determined by neutron diffraction at 4.2 and 115 K[7] and by *X*-ray diffraction at 295 K.[8] A charge-density analysis has been performed on data obtained at 120 K[8] and an essentially two-dimensional p.n.d. study has been carried out.[9] In addition, the magnetic behaviour of this[10] and a $P2_12_12_1$ polymorph[11] have been studied.

$[Fe(bipy)_2Cl_2][FeCl_4]$ is a salt composed of an approximately octahedral $Fe^{III}$ cation and an approximately tetrahedral $Fe^{III}$ anion as shown in the Figure. The two polymorphs differ in the details of the packing arrangement of these two ions. In the *Pccn* form both of the ions possess a two-fold axis long *c*, giving 25 atoms in the asymmetric unit, a small number for such a large system.

The high-spin $3d^5$ $Fe^{III}$ ions are weakly antiferromagnetically coupled, so that at a temperature of 4.18 K and a magnetic field of 4.62 T the magnetisation of the deuteriated material, with the field parallel to *b*, corresponds to 26.72(8) B.M. per unit cell.[12] This magnetisation is 65% of the saturation value, and is sufficient for the purposes of the p.n.d. experiment. The interionic magnetic exchange coupling, as revealed in the previous p.n.d.[9,10] and Mössbauer[11] (other polymorph) results is complex. The independent $Fe^{III}$ atoms in the cation and in

† *Supplementary data available* (No. SUP 56690, 10 pp.): magnetic structure factors, spin density parameters. See Instructions for Authors, *J. Chem. Soc., Dalton Trans.*, 1988, Issue 1, pp. xvii—xx.

*Non-S.I. units employed:* B.M. = $9.27 \times 10^{-24}$ J $T^{-1}$, e = $1.602 \times 10^{-19}$ C.

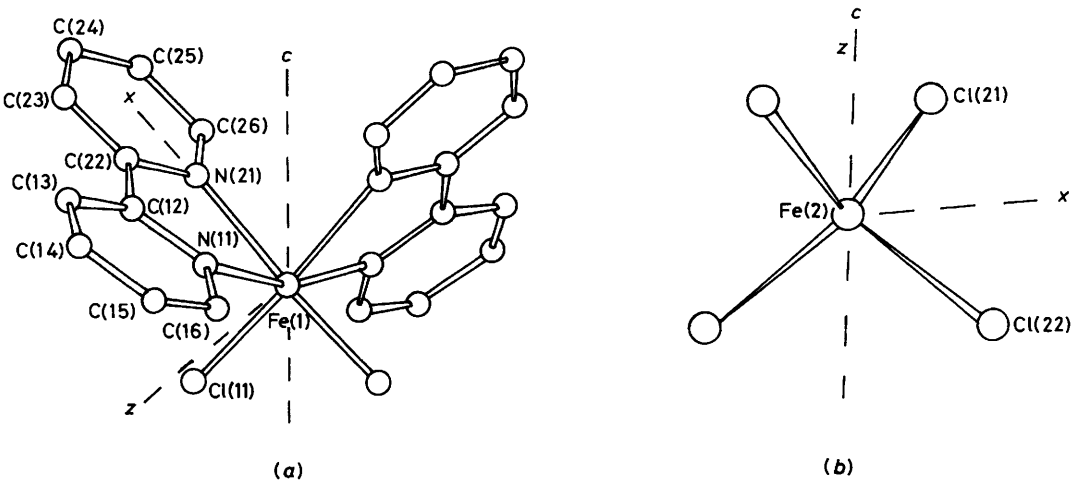


**Figure.** Structure of (*a*) $[Fe(bipy)Cl_2]^+$ and (*b*) $[FeCl_4]^-$

the anion possess substantially different magnetisations, and the bulk magnetisation is anisotropic. Due to the limited nature of the earlier p.n.d. data, it could not be interpreted at as high a level as the charge-density data.

In this paper we present further p.n.d. data, obtained to complement those of the earlier experiment[9] and correct its deficiencies. Now both the *X*-ray and p.n.d. experiments may be analysed at the same level to examine anisotropic components in the spin and charge densities around the atoms within the complex.

The charge-density analysis provided results which may be summarised as follows. (*i*) The three independent $Fe^{III}$–Cl bonds, in both the tetrahedral and the octahedral iron atoms, all show a donation, mainly of σ-symmetry, of *ca.* 0.7 e, to an iron atom. (*ii*) The $Fe^{III}$–N(bipy) bonds show a π back-donation of *ca.* 0.4 e from the iron atom onto the relevant pyridine ring. (*iii*) The iron atom in the $[FeCl_4]^-$ anion has a lower net charge [+0.8(3) e] due to a larger diffuse orbital population than that in the $[Fe(bipy)_2Cl_2]^+$ cation, which remains close to the formal value of 3 e [2.6(3) e]. (*iv*) The charge densities around the chlorine ligand atoms are substantially perturbed, probably by 'intermolecular' effects.

Ignoring conclusions relating to the magnetic coupling, the earlier spin-density analysis, which was interpreted only in terms of spherical atom densities, showed that: (*i*) each $Fe^{III}$–Cl bond leads to *ca.* 0.2 spins on the Cl atom; (*ii*) 0.1 spins appear on each nitrogen atom, with little on the remainder of the relevant pyridine ring; (*iii*) there is little diffuse spin population on the iron atom in either the cation or the anion; and (*iv*) the spin density in the $Fe^{III}$–Cl bonds is very small at the mid-bond position, indicating that the spin is mainly in antibonding molecular orbitals.

Simple ligand-field type models, with 'spin-paired' molecular orbitals cannot accommodate all these observations simultaneously, although they may be predicted individually.[8] Models allowing electron–electron correlation, such as unrestricted Hartree-Fock (UHF), configuration-interaction Hartree-Fock (CIHF), or $X\alpha$, are required to interpret the experiments fully, just as they are in less complex systems.[1,3] This requirement, well known in the applications of *ab initio* theory, appears naturally in the diffraction experiment results, but is difficult to demonstrate *via* spectroscopy.

We now proceed to an analysis of a fully three-dimensional p.n.d. data set on $[Fe(bipy)_2Cl_2][FeCl_4]$ to amplify these earlier conclusions.

## Experimental

A brown transparent crystal of 90(2)% deuteriated orthorhombic *Pccn* $[Fe(bipy)_2Cl_2][FeCl_4]$, $a = 1.497(2)$, $b = 1.224(2)$, $c = 1.321(2)$ nm, prepared as described previously,[9] was mounted on the D3 normal-beam polarised neutron diffractometer at the high-flux reactor of the Institut Laue-Langevin, Grenoble. The *b* axis was set a few degrees off the vertical axis of the diffractometer, so as to minimise the multiple scattering effects. The crystal was a plate of dimensions 2.2 × 4.5 × 1.9 mm ([100] × [010] × [001]) and weighed 33.2 mg. The previous experiment,[9] with *c* almost vertical, gave 206 unique magnetic structure factors with resolution good in *a* and *b* but poor in *c*. This new experiment was designed to give resolution good in *a* and *c* although poor in *b*, thus complementing our previous data and leading to good resolution in all the principal axes.

The D3 diffractometer measures flipping ratios for each reflection, equation (1), where $I_\uparrow$ and $I_\downarrow$ are the measured

$$R(hkl) = I_\uparrow(hkl)/I_\downarrow(hkl) \quad (1)$$

intensities at the Bragg peaks when the neutron polarisation is parallel and antiparallel, respectively, to the (vertical) magnetic field. For a centrosymmetric crystal one obtains from the flipping ratio the magnetic structure factor $F_M(hkl)$ defined in both magnitude and sign by expression (2). Here $F_N(hkl)$ is the

$$F_M(hkl) = F_N(hkl)\{U \pm [U^2 - \sin^{-2}\alpha]^{\frac{1}{2}}\} \quad (2)$$

nuclear structure factor obtained from an *unpolarised* neutron diffraction experiment, $U = [R(hkl) + 1]/[R(hkl) - 1]$, and α is the angle between the scattering vector for reflection *h,k,l* and the magnetic field direction.[13] In practice, further experimental corrections for imperfect flipping efficiency and incomplete beam polarisation must be applied.[14]

The previous neutron structure determination, on a crystal from the same batch, showed no extinction.[7] The final model fitting to the new data, discussed below, also showed no signs of extinction in the reflections of high scattered intensity. Reflections corresponding to a small value of $F_N(hkl)$ were not measured as they are susceptible to large errors, probably on account of multiple scattering effects.[1]

At 4.21(1) K, a magnetic field of 4.62(1) T, and a wavelength of 92.40(3) pm the flipping ratios of 921 reflections were measured, some more than once. They comprised a set of all

**Table 1.** Quantization axes and hybrid orbitals used in the anisotropic refinement

| Atom | *z* axis | *x* axis | Hybrids |
|---|---|---|---|
| Fe(2) | *c* | → [Cl(21) + Cl(22)]/2 | 5 × 3*d*, 3 × 4*p* |
| Cl(21) | in plane of Fe(2)–Cl(21)–Cl(21′) | → Fe(2) | 2 × *sp*, 2 × $3p_\pi$ |
| Cl(22) | in plane of Fe(2)–Cl(21)–Cl(22′) | → Fe(2) | 2 × *sp*, 2 × $3p_\pi$ |
| Fe(1) | N(21) | → *c* | 5 × 3*d*, 3 × 4*p* |
| Cl(11) | in Cl(11)–Fe(2)–N(11) plane | → Fe(1) | 2 × *sp*, 2 × $sp_\pi$ |
| N(11) | in plane of ring 1 | → Fe(1) | 3 × $sp^2$, 1 × $2p_\pi$ |
| N(21) | in plane of ring 2 | → Fe(1) | 3 × $sp^2$, 1 × $2p_\pi$ |
| C(12)—C(25) | *y* perpendicular to ring | | 1 × $2p_\pi$ |
| ov(lig) | | | 1 × '1*s*' |

accessible reflections with $F_N(hkl) > 10^{-13}$ m to a $\sin\theta/\lambda$ maximum of 7.00 $nm^{-1}$.

For each reflection equation (2) was solved to obtain $F_M(hkl)$. The choice of sign in equation (2) was always clear provided that it was accepted that most of magnetisation was 3*d*-like and centred on an iron atom. The equivalent reflections were averaged to give a final set of 196 unique *H*-‖-*b* magnetic structure factor data. The errors assessed for these data include an estimate of the error in the value of $F_N(hkl)$ obtained from the structure determination as well as the counting statistics. The agreement between equivalent reflections was consistent with the counting statistics as the determining source of error.

Together with the 206 *H*-‖-*c* data we have available a final data set of 403 reflections if we include the value of $F_M(000)$ obtained from the measurement of the magnetisation along *b*.

*Modelling the Data.*—To fit the magnetic structure factors to a model for the spin density within the crystal requires an estimate of the effects of orbital magnetisation and of magnetic saturation. The $Fe^{III}$ ion possesses the $^6A_{1g}$ ground term in a crystal field of cubic symmetry, and the e.s.r. *g* parameter for that term is well established to be 2.00, corresponding to the spin-only value. Consequently, the orbital magnetisation contributions to the $F_M(hkl)$ are zero.

As in previous cases, we can model the spin density using a magnetisation density model. Unlike previous cases, this crystal possesses two crystallographically independent and chemically distinct sites containing large amounts of spin, and they have different magnetic saturation behaviours. These features complicate the conversion of magnetisation to spin. In any crystal which is not fully magnetically saturated the ratio of spin to magnetisation density is, in principle, not constant throughout the crystal. Because the amount of spin on ligand atoms in transition-metal co-ordination complexes is small, it is normally sufficient to assume that the ratio exactly follows that on the main metal site. In the present case we have *two* iron atom sites with different ratios. It is reasonable, although not rigorous, to use the ratio for the Fe atom in each site to apply to the ligands bonded to it: thus we have one ratio within the $[Fe(bipy)_2Cl_2]^+$ unit and another within the $[FeCl_4]^-$ fragment. Since the crystal is magnetically anisotropic[10] we must model two such saturation ratios for each of the *H*-‖-*b* and *H*-‖-*c* data sets. Our magnetisation model has, then, four magnetic saturation parameters. Having a model for the spin density on each unit, we can calculate the Fourier components of the total magnetisation density, $F_M(hkl)$, using just these four extra parameters.

The crystal is complex and we therefore chose to model the spin density in terms of chemically important parameters, a 'valence' model. While such a model is not as complete as a full multipole analysis we have shown elsewhere[15] that those multipoles *not* included in the chemically based valence analysis probably have very little significance in the fit. In the present case the number of data is insufficient to support a multipole analysis since the number of multipole parameters required is much larger than for the valence model.

The spin model chosen is almost identical to that used for the charge-density analysis, a few parameters not appropriate for a spin density being omitted. On each iron atom we place five 3*d* orbitals and three 4*p* orbitals. The quantisation axes for these orbitals are given in Table 1. For Fe(2) we chose the local axes defined by the ligand atoms, one of which is the two-fold symmetry axis. On Fe(1) the quantisation axes use the two-fold crystallographic symmetry axis. On each chlorine atom we use a $3p_\sigma$ and two $3p_\pi$ orbitals, on each nitrogen atom an $(sp^2)_1$ 'lone pair' hybrid orbital directed at Fe(2), two further such hybrid orbitals, $(sp^2)_2$ and $(sp^2)_3$, directed at carbon atoms, and a $2p_\pi$ orbital appropriate for the π-orbital system of the pyridine ring. The carbon atoms are assigned $2p_\pi$ orbitals. In addition we place at the mid-point of each iron donor-atom bond a function, labelled ov(lig) with the radial dependence of a hydrogen 1*s* orbital and thermal motion the average of iron and ligand atoms, to model iron–donor atom overlap spin density. Also, since a large amount of spin is expected in the Fe 3*d* orbitals, we have refined parameters reflecting the 3*d* orbital radial dependences. We also allowed for radial dependence of the 4(*s*/*p*)-like density on Fe(1). The values for these parameters, $\kappa_{nl}$, reflect a linear expansion ($\kappa > 1$) or contraction ($\kappa < 1$) of the scattering curves for the orbital concerned.

Such a model still involves a large number of parameters. The number was reduced by introducing constraints on the relationships between the ring carbon atom populations. We initially assumed that (*i*) the two pyridine rings of a bipyridyl ligand molecule are different, but that (*ii*) the two sides of each pyridine are identical. That is, C(12) = C(16), C(13) = C(15), C(22) = C(26), C(23) = C(25).

The scattering curves employed were taken from a standard tabulation,[16] except for iron where the functions were calculated using the program ATOMSCF[17] for the configuration (Ar core)$3d^5 4p^1$. The 43 variables of the model refined on the 403 data to give a goodness-of-fit, $\chi$, of 1.56, $R(F) = 0.057$, $R'(F) = 0.052$, $F_M(000)$(calc.) = 26.72 B.M. We label this refinement R1. A list of observed and calculated magnetic structure factors corresponding to this refinement are given in SUP 56690.

Since some of the features of this model are arbitrary, we have performed several variations of it, changing one feature at a time, as follows.

R2: Obtained by adding 1*s* functions on all eight hydrogen atoms of the 2,2′-bipyridyl ligand molecule, produced only a small improvement in fit; $\chi = 1.52$. In this fit there was negative correlation between the H 1*s* populations and the populations

on the parent carbon atom, and that is the basis of the C and H population association seen in the earlier study.[9] However in this three-dimensional refinement no hydrogen-atom populations were significantly different from zero, in contrast to the earlier two-dimensional spherical-atom treatment.

R3, R4: Obtained by releasing the carbon 2*p* population constraints, or by using 2*s* orbitals on carbon atoms, produced almost no improvement in fit; $\chi = 1.55$ and 1.60.

R5, R6: Obtained by increasing the carbon atom population constraints so that C(13) = C(23) = C(15) = C(25), C(12) = C(22) = C(16) = C(26), and C(14) = C(24), gave a significantly poorer fit, as did setting the carbon atom populations all at zero; $\chi = 1.62$ and 1.64.

R7: Omitting the mid-bond overlap populations gave a significantly poorer fit; $\chi = 1.64$.

R8: Constraining the populations of the 3*d* orbitals on Fe(2) to conform to cubic symmetry ($d_{xy} = d_{xz} = d_{yz}d_{z^2} = d_{x^2-y^2}$) gave no improvement in fit; $\chi = 1.56$.

R9: Constraining the two sets of three 4*p* populations on the $Fe^{III}$ atoms to be equal gave a significantly poorer fit; $\chi = 1.65$.

R10: Allowing the $p_\pi$ orbital populations on chlorine to be unequal produced no appreciable improvement in fit; $\chi = 1.56$.

R11: On changing the choice of quantisation axes on Fe(1) from the *a*, *b*, and *c* crystal axes to local axes defined by Cl(11) and N(21) no improvement in fit was observed; $\chi = 1.59$.

The spin populations and other results corresponding to refinement R1 are given in Table 2. For the *H*-||-*b* data we deduce 81(1)% saturation at the Fe(1) site and 52(1)% saturation at the Fe(2) site. For the *H*-||-*c* data the figures were respectively 72(1) and 51(1)%. The net spin populations obtained are consistent with the results of the previous spherical-atom level refinement on part of this data.[9] A summary of the net spin populations is given in Table 3, together with the pertinent charge-density analysis results.[8]

The results of refinements R1 to R11 are given in SUP 56690.

**Table 2.** The spin density parameters* from refinement R1 in $[Fe(bipy)_2Cl_2][FeCl_4]$

| | | | | | |
|---|---|---|---|---|---|
| $[Fe(bipy)_2Cl_2]^+$ cation | | | | | |
| Fe(1) | $3d_{xy}$ | 0.82(8) | N(11) | $(sp^2)\sigma$ | 0.03(3) |
| | $3d_{xz}$ | 0.91(7) | | $2p_\pi$ | 0.10(2) |
| | $3d_{yz}$ | 0.84(6) | N(21) | $(sp^2)\sigma$ | 0.01(2) |
| | $3d_{x^2-y^2}$ | 0.84(8) | | $2p_\pi$ | 0.09(1) |
| | $3d_{z^2}$ | 0.97(8) | C(12) | $2p_\pi$ | −0.01(1) |
| | $4p_x$ | 0.09(16) | C(13) | $2p_\pi$ | −0.01(1) |
| | $4p_y$ | −0.97(16) | C(14) | $2p_\pi$ | −0.01(1) |
| | $4p_z$ | 0.28(22) | | | |
| | $\kappa_{3d}$ | 0.98(1) | C(23) | $2p_\pi$ | 0.01(1) |
| | $\kappa_{4p}$ | 1.09(6) | C(24) | $2p_\pi$ | 0.06(1) |
| | | | ov(11) | (1*s*) | −0.04(2) |
| Cl(11) | 3*p* | 0.15(2) | ov(N1) | (1*s*) | 0.00(2) |
| | $3p_\pi$ | 0.12(2) | ov(N2) | (1*s*) | 0.03(2) |
| $[FeCl_4]^-$ anion | | | | | |
| Fe(2) | $3d_{xy}$ | 0.80(9) | Cl(21) | $3p_\sigma$ | 0.13(4) |
| | $3d_{xz}$ | 0.80(6) | | $3p_\pi$ | 0.16(4) |
| | $3d_{yz}$ | 0.86(9) | | | |
| | $3d_{x^2-y^2}$ | 0.86(9) | Cl(22) | $3p_\sigma$ | 0.15(4) |
| | $3d_{z^2}$ | 0.80(9) | | $3p_\pi$ | 0.11(4) |
| | $4p_x$ | 0.45(21) | | | |
| | $4p_y$ | 0.41(21) | ov(21) | (1*s*) | −0.14(3) |
| | $4p_z$ | 0.19(22) | | | |
| | $\kappa_{3d}$ | 1.00(1) | ov(22) | (1*s*) | −0.09(3) |

* The parameters are in spin units, except for $\kappa_{nl}$ which are dimensionless. ov(*n*) Refers to the overlap in the Fe–Cl(*n*) bond, ov(N1) and ov(N2) to overlap in Fe–N(11) and Fe–N(21) bonds respectively.

## Discussion

*Bonding.*—In the $[FeCl_4]^-$ ion unpaired electrons occupy both the $e^*$ and $t_2^*$ molecular orbitals (m.o.s) which are respectively π and (π + σ) antibonding in character. Spin is transferred to the chlorine atoms *via* these m.o.s. In simple spin-paired models, where the distribution of up-spin and of down-spin is identical, our full data set allows us to divide the spin between the $e^*$ and $t_2^*$ orbitals in the following way. We assume that, as simple l.c.a.o. (linear combination of atomic orbitals) theory predicts, the spin transfer by π interaction in the $e^*$ orbital is half that in the $t_2^*$ orbital. We then distribute the overlap populations so that each m.o. contains a single spin keeping the π overlap much lower in magnitude than the σ overlap. In addition, the 4*p* orbitals participate only in the $t_2^*$ orbital.

The $e^*$ orbitals thus contain 1.66 Fe(*d*), 0.36 Cl($3p_\pi$), and −0.02 π-overlap spins. The $t_2^*$ orbitals contain 2.46 Fe(3*d*), 0.23 Fe(4*p*), 0.18 Cl($3p_\pi$), 0.56 Cl($3p_\sigma$), and −0.43 (σ + π)-overlap spins. We can see that the spin-density results are just those that simple m.o. theory might predict. In particular we note that the chlorine atom engages in σ bonding more strongly than in π bonding, but that the total spin transfers *via* σ and π bonding are comparable because of the larger number of π-antibonding molecular orbitals (5π *versus* 3σ). The stronger σ bonding does *not* give an anisotropy in the 3*d* population, with $3d(t_2) > 3d(e)$, because this effect is counterbalanced by a substantial 4*p* population in the $t_2^*$ orbital. Lastly, as expected, the π overlap is close to zero, while the σ overlap (in $t_2^*$) is significantly negative. The overall covalence is large: 22% of the spin is localised on the chlorine atoms.

In studies on the $[CoCl_4]^{2-}$ ion using p.n.d.[1] and *X*-ray

**Table 3.** A summary of the spin density and the charge density results.[8] The 3*d* and 4*p* + ov charge results for $Fe^{III}$ atoms are populations, not net charges

| Atom | | Charge | Spin | Unit | Charge | Spin |
|---|---|---|---|---|---|---|
| Fe(1) | 3*d* | 5.5(2) | 4.38(15) | C; ring 1 | 0.37(8) | −0.04(1) |
| | 4*p* + ov | 0.0(3) | −0.60(15) | C; ring 2 | 0.37(8) | 0.15(2) |
| | Total | 2.56(3) | 3.78(17) | bipy; ring 1 | −0.29(8) | 0.09(3) |
| Cl(11) | | −0.20(6) | 0.25(3) | bipy; ring 2 | −0.45(8) | 0.25(3) |
| N(11) | | −0.66(5) | 0.13(2) | | | |
| N(21) | | −0.82(4) | 0.11(2) | | | |
| Fe(2) | 3*d* | 5.7(2) | 4.13(5) | | | |
| | 4*p* + ov | 1.5(3) | 0.0(17) | | | |
| | Total | 0.83(30) | 4.13(16) | | | |
| Cl(21) | | −0.33(6) | 0.22(4) | | | |
| Cl(22) | | −0.41(5) | 0.22(4) | | | |

diffraction[14] and by theory,[18,19] we have noted that spin or charge densities can be separately interpreted to fair accuracy employing simple spin-paired m.o. models. However, they cannot be so interpreted consistently with each other. The covalence parameters for the charge density are greater than those from the spin density. This difference is due to the neglect of electron–electron correlation which causes spin polarisation. The effect is that charge-based parameters overestimate the amount of spin delocalised onto the donor atoms of the ligands. We also see that effect here: while 1.1 spins have been transferred to the ligands, 2.2 units of charge have been donated to the Fe(2) atom. This discrepancy is too large to be accounted for by differences in normalisation constants between the bonding and corresponding antibonding molecular orbitals, which do make transferred charge slightly larger than spin in simple spin-paired models. It is also difficult to account for the much larger 4*p* participation deduced in the charge-density analysis using only a simple model.

We must conclude that, as in previous cases studied,[3] the bonding in the $[FeCl_4]^-$ ion shows effects due to electron–electron correlation of a similar size to those arising from simple covalent spin transfer. This fact is not apparent from a study of the p.n.d. or charge-density results in isolation, but only in their combination. Theoretical studies on the $[CoCl_4]^{2-}$ ion support this conclusion,[1] although the agreement between theory and experiment is not quantitative.

*Bonding in the* $[Fe(bipy)_2Cl_2]^+$ *Ion.*—The $Fe^{III}$–Cl bond in the cation is very similar to that in the $[FeCl_4]^-$ anion. The σ bonding is greater than, although comparable with, the π bonding, and the total spin transferred is 0.27 per chlorine atom, with an overlap population of −0.04 spins. As expected, the antibonding orbitals $e_g^*(\sigma)$ and $t_{2g}^*(\pi)$ are involved.

The bonding to the 2,2′-bipyridyl molecule is more complex. Previously[9] the data could only support the conclusions that less spin is delocalised onto each pyridine ring than onto the chlorine atoms, and that most of it resided on the nitrogen atoms. The new data are sufficient to allow us to arrive at the following conclusions. (*i*) Fe–N bonding for ring 1 is *different* from that for ring 2; *cf.* refinements R5 and R1. (*ii*) Within each ring the left and right hand halves are not significantly different from each other; *cf.* refinements R3 and R1. (*iii*) The spin on the carbon atoms is significant in magnitude; *cf.* refinements R6 and R1.

However the precise distribution of spin on each carbon and hydrogen atom is not so well defined. We have assumed the spin occupies only carbon $2p_\pi$ orbitals. This is reasonable if the spin is restricted to the ligand molecule π and π* orbitals, where simple considerations place it. However, if there is spin polarisation we may expect functions of σ symmetry, such as C ($sp^2$) hybrids and the H 1*s* orbitals also to carry spin. Ring 1 carries only 0.09(3) spins, 0.13(2) on the nitrogen donor atom and −0.04(1) on the remaining atoms. The small amount of delocalisation concerning this nitrogen atom suggests that the Fe(1)–N(11) bond is predominantly σ in character. The nitrogen atom orbital populations, however, suggest appreciable π interaction. The Fe–N overlap population, 0.00(1) spins, suggests a balance of π bonding and σ antibonding interactions in half-occupied orbitals. Taken together, our results suggest that *ca.* 0.07 spins are delocalised in the σ-antibonding orbitals and *ca.* 0.07 in a π-bonding orbital.

Ring 2 carries 0.25(3) spins, with substantial delocalisation, 0.15(2) spins, away from the nitrogen atom, suggesting much stronger π bonding than for ring 1. The positive Fe–N overlap population also suggests that π bonding is much more dominant than σ antibonding in this spin-density region. We can predict that the π interaction is with pyridine-based low energy π* or π orbitals. *Ab-initio* STO-3G basis set calculations undertaken on pyridine employing the program Gaussian-70[20] showed only one accessible π* orbital with a significant coefficient on the nitrogen atom. The nitrogen, *ortho*-, *meta*-, and *para*-carbon atom coefficients were found to be 0.64, −0.34, −0.31, and 0.67. There is a suitable π orbital with coefficients 0.52, 0.22, −0.03, and −0.54. Thus if there is π interaction we expect spin mainly on the nitrogen and C(24), the *para*-carbon atom of ring 2. The largest carbon atom spin population of 0.06(1) is indeed found on C(24). Taken together, we can interpret our results as *ca.* 0.07 spins σ donated from Fe(1) onto the nitrogen atom *via* an antibonding orbital together with *ca.* 0.2 spins on the ligand in a π-bonding orbital. The metal $3d_\pi$ orbitals can interact with either π or π* orbitals but, in contrast to the charge case, the spin involves an antibonding or bonding orbital respectively. The overlap populations seem to indicate spin in *bonding* orbitals, *i.e.* π back-donation of spin (and charge) from Fe($3d_\pi$) into π* orbitals.

Given the small Fe–N bond length difference, Fe(1)–N(21) 214.6, Fe(1)–N(11) 217.0 pm, the larger spin transfer for ring 2 than for ring 1 is unlikely to be a consequence. More probably, a '*trans* effect' by the chlorine *versus* nitrogen ligand across the Fe–N bond is responsible, although it may be difficult to quantify such a suggestion.

The comparison of the charge with the spin-density results shows a similar pattern to that of the $[FeCl_4]^-$ anion; there is qualitative agreement but quantitative disagreement in the direction expected for correlation effects. In particular from the charge distribution we notice that metal–ligand π back-bonding seems stronger than σ antibonding for both rings and in addition is the greater in ring 2, −0.45(8) *versus* −0.29(8) e for ring 1, in agreement with the p.n.d. conclusions, particularly with the view that there is π back-donation from metal to ligand.

*Relationship between Spin and Magnetisation Densities.*—The magnetisation densities with *H*-‖-*b* and with *H*-‖-*c* and the spin density are not simply interrelated in the present crystal unless certain approximations are made. In particular we assume that we are dealing with $[FeCl_4]^-$ and $[Fe(bipy)_2Cl_2]^+$ ions with separate degrees of magnetic saturation within each ion. One model for that is appreciable magnetic exchange within two sub-lattices in the crystal but not between them. This picture is belied by the complex magnetic behaviour of the crystals at the lowest temperatures, showing the effects of the very small inter-lattice exchange.[10,11] However, the excellent fit with our four magnetisation parameters shows that the independent saturation approximation is good at 4.2 K, even though our data are sufficiently precise that we are able to detect some deficiencies in the model as outlined below.

We refined our valence orbital population model using the *H*-‖-*b* and *H*-‖-*c* data separately. We took care, since each data set is of limited resolution along the direction parallel to the magnetic field, not to vary ill defined parameters. Thus we used spherical 2*s* orbitals on N and 3*s* on Cl and fixed Fe(1) $3d_{x^2-y^2}$ and Fe(2) $3d_{z^2}$ in the *H*-‖-*c* and Fe(1) $3d_{z^2}$ and Fe(2) $3d_{x^2-y^2}$ populations in the *H*-‖-*b* data. The two data sets give, within the somewhat larger errors, the same results for the refined parameters as the combined treatment, with one exception. We found that the Fe(1)-centred diffuse 4*p* density in the $[Fe(bipy)_2Cl_2]^+$ ion changes significantly between the refinements. The $4p_y$ population, −0.07(25), is not significant for the *H*-‖-*c* data but large and negative, −1.29(15), for the *H*-‖-*b* data. The lobes of the $4p_y$ orbital are directed almost along the [110] direction. It seems that we are seeing a more subtle effect of the magnetic exchange than just saturation of two independent sites. However, there is no evidence that the less diffuse components of the spin density such as the $Fe^{III}$ 3*d* or ligand *s* and *p* orbital populations are affected in a similar fashion.

The magnetic exchange in a low-symmetry crystal such as the

present one is a very complicated phenomenon and there is no chance that a complete account of it could be achieved on the basis of the magnetic susceptibility and magnetisation data available to us, even though these are more extensive than is common in relationship to p.n.d. studies on paramagnetic systems. While it would be reassuring to have a complete description of the magnetic exchange in the crystal, the effects of that exchange are so small that we can proceed on the individual site-saturation model with confidence, except to some extent for the diffuse iron-centred populations. They are the ones most likely to be involved in conveying magnetisation information from one of the sub-lattices to the other.

## Conclusions

The extension of the p.n.d. data set from near two-dimensional to three-dimensional for this high-magnetisation crystal has allowed a good analysis of the chemical bonding to the iron atoms in a fairly large system. We are confident that our data and its analysis can be of sufficient quality to allow us to make worthwhile studies on other many-atom systems. Suitable compounds may include some with relationship to biologically important molecules; an experiment on (5,10,15,20-tetraphenylporphyrinato)iron(III) chloride is in preparation.

## Acknowledgements

We thank the Australian Research Grants Scheme for financial support and the Institut Laue-Langevin, Grenoble, for access to the D3 diffractometer.

## References

1 G. S. Chandler, B. N. Figgis, R. A. Phillips, P. A. Reynolds, R. Mason, and G. A. Williams, *Proc. R. Soc. London, A*, 1982, **384**, 31.
2 P. Day, P. J. Fyne, E. Hellner, M. T. Hutchings, G. Munninghoff, and F. Tasset, *Proc. R. Soc. London, A*, 1986, **406**, 39.
3 B. N. Figgis, J. B. Forsyth, and P. A. Reynolds, *Inorg. Chem.*, 1987, **26**, 101.
4 G. A. Williams, B. N. Figgis, and R. Mason, *J. Chem. Soc., Dalton Trans.*, 1981, 734.
5 B. N. Figgis, G. A. Williams, J. B. Forsyth, and R. Mason, *J. Chem. Soc., Dalton Trans.*, 1981, 1837.
6 B. N. Figgis, J. M. Patrick, P. A. Reynolds, B. W. Skelton, A. H. White, and P. C. Healey, *Aust. J. Chem.*, 1983, **36**, 2043.
7 B. N. Figgis, P. A. Reynolds, and N. Lehner, *Acta Crystallogr., Sect. B*, 1983, **39**, 711.
8 B. N. Figgis, P. A. Reynolds, and A. H. White, *Inorg. Chem.*, 1985, **24**, 3762.
9 B. N. Figgis, P. A. Reynolds, and R. Mason, *Inorg. Chem.*, 1984, **23**, 1149.
10 B. N. Figgis, E. S. Kucharski, and P. A. Reynolds, *Aust. J. Chem.*, 1983, **36**, 2369.
11 E. H. Witten, W. M. Rieff, K. Lazar, B. W. Sullivan, and B. M. Fox, *Inorg. Chem.*, 1985, **24**, 4585.
12 J. B. Forsyth, unpublished work.
13 W. Marshall and S. W. Lovesey, 'The Theory of Thermal Neutron Scattering,' Oxford University Press, 1971.
14 P. J. Brown and J. B. Forsyth, *Br. J. Appl. Phys.*, 1964, **15**, 1529.
15 B. N. Figgis, P. A. Reynolds, and A. H. White, *J. Chem. Soc., Dalton Trans.*, 1987, 1737.
16 'International Tables for *X*-Ray Crystallography,' eds. J. A. Ibers and W. C. Hamilton, Kynoch Press, Birmingham, vol. 4, 1974.
17 B. Roos, C. Salez, A. Veillard, and E. Clementi, 'I.B.M. Research Report,' I.B.M. Research Laboratories, San Jose, RJ518, 1968.
18 H. Johansen and N. K. Andersen, *Mol. Phys.*, 1986, **58**, 965.
19 L. A. Barnes, G. S. Chandler, B. N. Figgis, and K. Fujima, unpublished work.
20 W. J. Hehre, W. A. Lathan, R. Ditchfield, M. D. Newton, and J. A. Pople, Quantum Chemistry Program Exchange, 1965, vol. 10, program no. 236.

*Received* 18*th November* 1986; *Paper* 6/2224